Mechanical and microstructural properties of fly ash-based engineered geopolymer mortar incorporating waste marble powder

by

Parmender Gill
Scholar, Department of Civil Engineering, DCRUST, Murthal, (Sonepat). Haryana, India.
Email: *parmender.schcivil@dcrustm.org*

Vijaya Sarathy Rathanasalam
Associate Professor, Atria Institute of Technology, Bengaluru -560024, Karnataka, India
Email: *rvsarathycivil@gmail.com*

Parveen Jangra (Corresponding author)
Assistant Professor, Department of Civil Engineering, DCRUST, Murthal (Sonepat), Haryana
Email: *separveenjangra@dcrustm.org*

Thong M Pham (Corresponding author)
UniSA STEM, University of South Australia, Mawson Lakes, SA, 5095, Australia.
Email: *thong.pham@unisa.edu.au*

Deepankar Kumar Ashish
School of Engineering, Cardiff University, Cardiff, CF24 3AA, UK
Department of Civil Engineering, Maharaja Agrasen Institute of Technology, Maharaja Agrasen University, Baddi, 174103, India.
Email: *deepankar1303@gmail.com*

Mechanical and microstructural properties of fly ash-based engineered geopolymer mortar incorporating waste marble powder

Parmender Gill[1], Vijaya Sarathy Rathanasalam[2], Parveen Jangra[1,*], Thong M. Pham[3,*], Deepankar Kumar Ashish[4]

[1]*Department of Civil Engineering, DCRUST Murthal-131039, Haryana, India.*

[2]*Department of Civil Engineering, Atria Institute of Technology, Bengaluru -560024, Karnataka, India*

[3]*UniSA STEM, University of South Australia, Mawson Lakes, SA, 5095, Australia.*

[4]*School of Engineering, Cardiff University, Cardiff CF24 3AA, UK.*

Email Corresponding authors: separveenjangra@dcrustm.org, thong.pham@unisa.edu.au

Abstract

The marble processing industry produces a large volume of unmanaged waste in the form of micro-fine marble particles, usually referred as waste marble powder (WMP). Unregulated and open disposal of WMP has adverse effects on the environment. Marble is usually rich in calcium content, which can be used in geopolymer technology thereby enhancing its recycling value. This research sought to determine the viability of WMP as a supplementary binder and polymerisation potential of its high calcium content (55.96%). For this purpose, WMP was used as fly ash replacement by weight (0, 5, 10, 15 and 20%) in geopolymer mortar (GPM) while other mix proportions are kept the same. The results indicated that WMP substitution adversely affected the water absorption (WA), ultrasonic pulse velocity (UPV), compressive and flexural strengths of engineered GPM. The mechanical strength trends were supported by, scanning electron microscopy (SEM), energy dispersive X-ray spectroscopy (EDS), X-ray diffraction (XRD) and Fourier transform infrared (FTIR) spectroscopy tests, which revealed that the calcium content of WMP showed poor alkali activation. Marble particles remained unreacted in the GPM matrix and failed to form additional geopolymeric compounds as Ca/Si ratio was found to consistently decrease with higher WMP substitution. Accordingly, WMP can be used in geopolymers in combination with siliceous binder (fly ash) without significantly reducing the mortar mechanical properties and thus the resulting GPM can find broad applications in practice.

Keywords: Waste marble powder, Geopolymer mortar, UPV, SEM, EDS, XRD, FTIR.

1. Introduction

Waste marble is a by-product of marble cutting and processing industry produced in the form of different sized aggregates and slurry. About 200 metric tons of marble waste are generated annually on a global scale, of which China accounts for 34%, followed by Italy (19%) and India (16%) (Pappu et al. 2019). Marble slurry contains micro-fine particles, commonly known as waste marble powder (WMP) when dried, constituting approximately 20% of the total marble waste (Khan et al. 2020). There is no systematic way to dispose of marble slurry and is usually dumped in nearby open spaces, resulting in soil pollution. The fine size of WMP reduces the permeability of topsoil which causes water logging. In addition, marble particles increase the alkalinity of soil, thus harming its productivity and loss of local greenery. Thus, there is a need to judiciously manage this non-biodegradable waste. This industrial by-product has been recycled in various applications such as brick manufacturing, landfills and road construction (Hebhoub et al. 2011).

Some researchers have shown the application of fine sized WMP in concrete manufacturing as a partial or complete replacement of sand to prevent the over-dependence and depletion of natural aggregates (Aliabdo et al. 2014; Ashish 2018; Ghani et al. 2020; Singh et al. 2017). Kabeer and Vyas (2018) have demonstrated that WMP could be successfully used to replace sand (up to 100%) in conventional cement mortar, with the optimum mix (20% WMP) showing an 84% increase in compressive strength. It was found in another study by Hebhoub et al. (2011) that the optimum compressive strength of 35.3 MPa can be obtained by replacing sand with 50% marble waste aggregates. The performance under parameters such as dry shrinkage and water absorption were found to be similar to the reference mix with natural sand. Generally, WMP exhibits higher density and Blaine's fineness than sand, enabling it to efficiently achieve a pore-filling effect in mortar and enhance mechanical properties such as porosity and density of the matrix structure (Ashish 2019).

In recent years, marble powder has also been investigated as a partial replacement to OPC in pastes and mortar, as WMP generally consists of high calcium oxide (30-60%) content and may present hydration potential. Comprehensive research was conducted by Ashish (2018) to investigate the feasibility of partial WMP replacement for OPC and sand amalgam. The author reported that when WMP was used as cement replacement, the 7-days compressive strength first increased by 7.17% for 10% WMP but then decreased by 6.77% for 15% WMP. Further,

EDX examination found a reduction in the elemental content of cementitious C_3S and C_2S compounds, which discredited WMP of any evident role in the hydration process. However, considering the substantial improvement in carbonation resistance, the author concluded that WMP could be used as a suitable additive in concrete. Vardhan et al. (2015) observed that the presence of WMP had a detrimental effect on the early hydration process, resulting in an increase in both the initial and final setting time. The observed decrease in compressive strength was attributed to the increase in number of voids with increase in WMP percentage from 10 to 50%, as determined through SEM images. Moreover, XRD investigation did not found any new compositions of cementitious phases. Instead, an increase in the intensity of crystalline peaks corresponding to calcite and Portlandite was detected. Other studies have also reported findings showing a decrease in mechanical strength when using more than 10 % WMP as a cement replacement in concrete or mortar (Wang et al. 2021; Lezzerini et al. 2022). However, some studies also revealed positive effects of WMP as cement paste replacement on early age (7-days) compressive strength of mortar. These effects were attributed to fluctuations in CaO and Fe_2O_3 content of WMP (Vardhan et al. 2019). According to Kumar et al. (2020), the observed densification of the concrete matrix in SEM pictures can be attributed to the filling effect of WMP particles, rather than any modification in pozzolanic activity. According to Arel (2016), the substitution of 5-10% of cement with marble dust would result in a 12% reduction in CO_2 emissions.

Geopolymer is a sustainable technology that harness the binding properties of industrial by-products, otherwise treated as waste and dumped, to produce a valuable construction material. This method requires activation of silicates and aluminates with an acidic or alkaline solution to form an inorganic polymeric chain (Palomo et al. 1999). Geopolymer mortar is an environmentally friendly construction material that is used as an alternative to greenhouse gas-emitting OPC-based products (Lee et al. 2016; Zhao et al. 2021). Despite its promising potential, active research is being conducted to assess the feasibility of other waste materials such as recycled aggregates that could enhance the mechanical strength and durability of the geopolymer composite structure (Gill et al. 2023, 2023).

There is a sufficient number of research studies which experimented on hydration potential of WMP in OPC-based mortar, but very limited studies have been done to explore the alkali activation potential of WMP in geopolymer-based mortar. Wang et al. (2011) indicated that dissolution of marble powder used as a replacement for natural aggregates could introduce

calcium-based compounds in geopolymer gel resulting in enhancement of the matrix strength. Saloni et al. (2021) examined employing utility of waste marble aggregates (WMA) as a partial substitute to natural coarse and fine aggregates (NA) in fly ash-based alkali activated concrete. In their study, the addition of 50% WMA increased the strength by formation of additional CASH gel, but pore microstructure deteriorated as reflected by deteriorating durability properties. Some researchers have attempted various ways to valorize marble powder as a potential precursor in rice husk ash and kaolin based geopolymers by combining it with cement, clay, gypsum and blast furnace slag, with limited success (Lee et al. 2020; Komnitsas et al. 2021; Kamseu et al. 2022; Kaya et al., 2022;).

Considering the high calcium content and lower percentages of silica and alumina (2 to 5%) in marble powder, a primary binder rich in amorphous silica and alumina content is necessary to support the development of inorganic C-A-S-H polymeric chain, based on geopolymer reaction mechanism (Duxson et al. 2007). Fly ash (FA) is a by-product of coal-fired thermal power plants and an established geopolymer precursor which contains high percentages of Al_2O_3 and SiO_2 (Saloma et al. 2016). Almost 370 million tonnes (MT) of FA is generated per year around the world (Dwivedi and Jain 2014). India and China, being the biggest producers of FA, produce about 112 MT and 100 MT of FA per year (Dwivedi and Jain 2014), respectively. However, geopolymer made from Indian fly ash, classified as low-calcium with less than 10% CaO, shows slow setting and low early-age strength (Chatterjee 2010; Rangan 2014; Jindal et al. 2017). This type of geopolymer requires heat curing to expedite the polymerisation process, which increases the overall production cost (Nath et al. 2015; Nikvar-Hassani et al. 2022). Incorporation of calcium-based products such as slag and OPC in FA based GPC has shown to significantly improve its mechanical and durability properties (Nath and Sarker 2015; Mehta and Siddique 2017, 2018). This study attempts to utilize the calcareous property of WMP in FA-GPM to gain similar benefits. Furthermore, fly ash availability for concrete sector is declining as it has shown advantageous application and cheap consumption in other construction fields such as road base construction, soil modification and structural fills among others (Alam and Akhtar 2014; Surabhi 2017; Yousuf et al. 2020).

Therefore, efforts to make use of other by-products such as WMP as contributing geopolymer binder are justified and indeed sought. Re-use of WMP in GPM would reduce material cost and enhance its sustainability measures. The purpose of this study is to cover the knowledge gap in this area and help identify WMP as a plausible precursor in geopolymer development.

This study investigates the polymerising potential of different MP-FA combinations (0, 5, 10, 15 and 20%) with Na_2SiO_3-NaOH alkali solution. Limited WMP replacement was experimented as excessive usage may lead to deterioration in properties of GPM, as learned from previous studies. The mechanical performance was judged based on water absorption, ultrasonic pulse velocity, compressive strength, and flexural strength tests. In addition, microstructural modifications were assessed by scanning electron microscopy, energy dispersive spectroscopy, X-ray diffraction and Fourier transform infrared spectroscopy.

2. Material and methodologies

2.1. Materials for geopolymer mortar

2.1.1. Fly ash and marble powder

The primary binder in this study is class-F fly ash which meets ASTM C 618 (2014) criteria . It was collected from a coal-fired power plant in Karnataka. The chemical composition of FA is summarised in **Table 1**. Fly ash particles have a spherical shape and they act as fillers resulting in a compact and denser morphology (Sinsiri et al. 2010). The concentration of silica in FA is 59.62%. Marble powder was acquired from processing facility situated near Panipat, India. As marble contains a high amount of calcium i.e., 55.96%, compounds which can provide great potential to generate additional gels in the mix such as calcium silicate hydrate (CSH) and calcium aluminate silicate hydrate (CASH) (Saloni et al. 2021b). These products are responsible for strength gain in the produced material.

Table 1. Chemical Composition of Fly ash & WMP

Chemical Composition	Fly Ash (%)	WMP (%)
Silica (SiO_2)	59.62	0.65
Alumina (Al_2O_3)	25.79	0.23
Iron Oxide (Fe_2O_3)	5.53	0.23
Total Sulfur (SO_3)	0.45	0.12
Calcium Oxide (CaO)	6.35	55.96
Potassium Oxide (K_2O)	1.23	0.16
Sodium Oxide (Na_2O)	0.31	0.14
Loss on Ignition (LOI)	0.72	42.51

XRD analysis also confirms the presence of amorphous silica in fly ash as the presence of quartz, mullite, mellite, and calcite can be seen in **Fig. 1 (a)** while the SEM image in **Fig. 1 (b)** shows the spherical shape of FA particles as reported in the literature. Marble powder had a

specific density of 2.76 which is much higher than 1.93 of fly ash particles as shown in **Table 2**. With a comparable mean particle size of 17 µm and Blaine fineness of 3728 cm^2/g, WMP can potentially replace FA in the mixes.

Table 2. Physical properties of fly ash and WMP

Properties	Fly ash	WMP
Specific density	1.93	2.76
Blaine fineness (cm^2/g)	3,918	3,728
Mean particle size (µm)	21	17

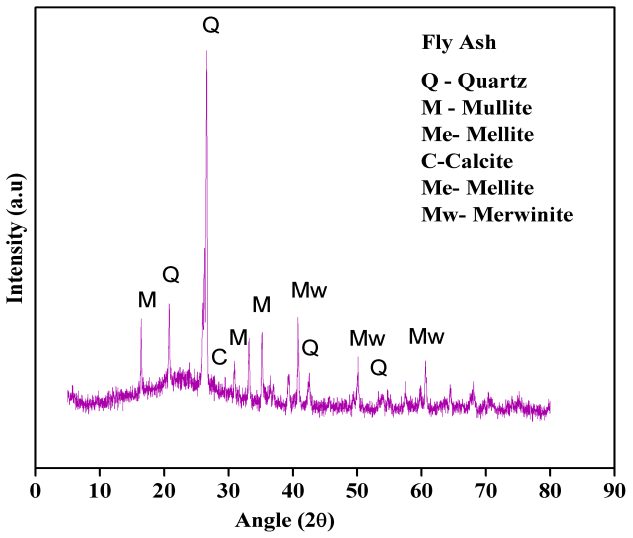

(a) XRD spectrum of fly ash

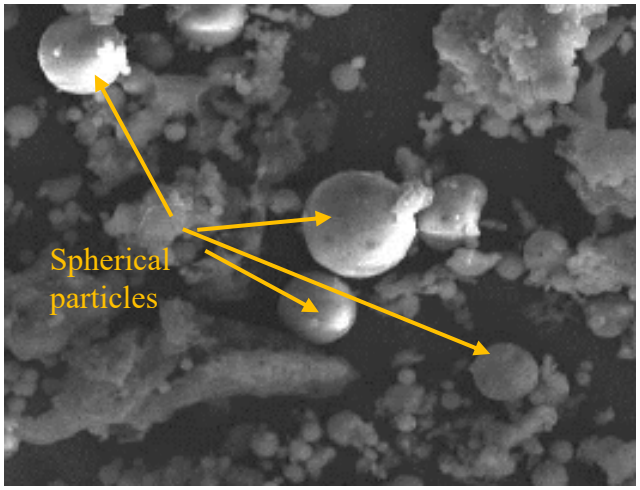

(b) SEM image of fly ash

Fig. 1. XRD spectrum and SEM image of fly ash.

2.1.2. Alkaline activator

By mixing 99% pure NaOH pellets with tap water, a solution of NaOH was prepared with 8M concentration. For producing an alkaline activator liquid (AAL), NaOH solution was mixed with sodium silicate (Na_2SiO_3) and was kept for 5 minutes. The ratio between Na_2SiO_3 and NaOH was 2.5 to achieve desirable outcomes as suggested in previous studies (Lloyd and Rangan 2010; Anuradha et al. 2012; Ferdous et al. 2013; Junaid et al. 2015). Preparation of this mixture was done 24 hours before the final mixing to reduce the excessive heat released when NaOH is combined with Na_2SiO_3.

2.1.3. Superplasticiser

Increased workability and flowability of the resultant mixture can be obtained by adopting a superplasticiser. In this study, a reducing agent polycarboxylate ether was used as a superplasticiser with water as suggested in a previous study (Ushaa et al. 2015).

2.1.4. Fine aggregates

Table 3 shows the chemical composition of Yamuna river sand procured from a local supplier, and utilized as fine aggregates. Natural fines were predominantly composed of silica (80.11%) and alumina (11.65%). All the physical properties of fine aggregates comply with requirements of ASTM C 33-13 (2013) and are shown in **Table 4**. For instance, specific gravity and water absorption of natural sand, (2.63 and 0.71%, respectively), fulfilled the ASTM C127 (2009) conditions. Sieve analysis of fine aggregates resulted in a fineness modulus of 2.82 and the particle size distribution (PSD) curve is shown in **Fig. 2**.

Table 3. Chemical composition of fine aggregates

Chemical Composition	(%)
Silica (SiO_2)	80.11
Alumina (Al_2O_3)	11.65
Iron Oxide (Fe_2O_3)	2.25
Calcium Oxide (CaO)	2.57
Magnesium Oxide (MgO)	0.44
Potassium Oxide (K_2O)	0.77
Sodium Oxide (Na_2O)	0.81
Loss on Ignition (LOI)	1.4

Table 4. Physical characteristics of fine aggregates

Physical Property	Fine Aggregates (%)	Limits [ASTM C33 (2013)]
Specific gravity (ASTMC127, 2009)	2.63	>2.5
Water absorption (%) (ASTMC127, 2009)	0.71	<1
Impact value (BS812-112, 2015)	16.3	<25
Crushing value (BS812-110, 1990)	19.8	<25
Abrasion test (ASTMC535, 2009)	26.7	<50
Bulk density (kg/m3) (ASTMC29/C29M, 1997)	1580	1200-1760
Voids content (%)(ASTMC29/C29M, 1997)	36.38	33-42

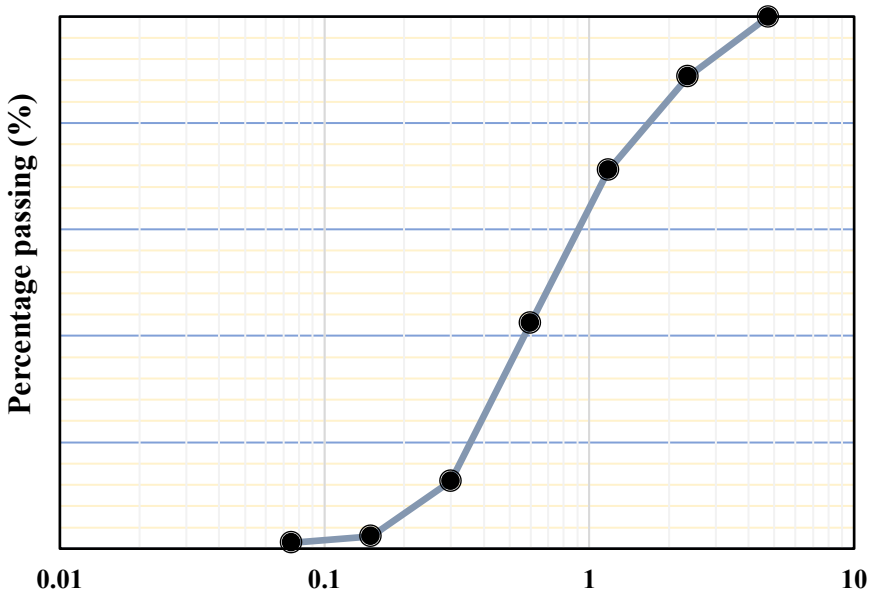

Fig. 2. PSD curve of fine aggregates used in the GPM mix.

2.2.Mix Proportion

Fly ash was used as the primary binder in all the GPM mixes while WMP was used as a supplementary binder. A total of five mixes were prepared as summarised in **Table 5.** The first mix 100F0M serves as a reference mix, in which "100F" indicates that the mix contains 100% FA and "0M" shows the percentage of WMP replacement (0% for reference mix). Other mixes had FA replaced by WMP with different percentages up to 20%.

Table 5. Mix Proportion

Mix ID	Fly Ash (gm)	Marble Powder (gm)	Sand (gm)	NaOH (gm)	Na_2SiO_3 (gm)	Extra Water (gm)	Plasticizer (gm)
100F0M	100	—	150	13	32	20	2
95F05M	95	5	150	13	32	20	2
90F10M	90	10	150	13	32	20	2
85F15M	85	15	150	13	32	20	2
80F20M	80	20	150	13	32	20	2

2.3.Mixing, casting and curing

All the materials were dry mixed using a pan mixer for around 5 minutes. Afterwards, the activator solution was added to the dry mixture. The mixes were then cured by heating in an oven for 24 hrs at about 60°C. Heat curing was adopted to obtain the maximum compressive strength as possible. To avoid evaporation of the samples, polyvinyl sheets were used to seal

all the samples. Next, all the samples were then stored in a laboratory until testing. The laboratory temperature was between 25° - 27°C.

2.4.Testing of specimens

2.4.1. Ultra-sonic pulse velocity test

ASTM C597 (2016) guidelines were adopted to conduct ultra-sonic pulse velocity (UPV) tests. A grinder was used to polish the faces of the cylindrical specimens. For the reception and transfer of ultrasonic waves, piezo-transducers were used. The first transmitter was connected to one end of the sample while the receptor transducer was attached to the other end. To eliminate air, lubricant was used. A standard plastic bar of cylindrical shape having fixed values of the wave velocity was used for equipment calibration before each experiment, which helps in attaining proper readings.

A digital device triggered an actuator (JSR DPR 300). Picoscope V6.4.64.0 was used for processing the datagrams. Time (t) taken by the pulse to pass through the sample was monitored by a detecting sensor on a digital metre. This time is known as the 'time of flight'. When both of the transducers were placed at the centre of the specimen, the acoustic pulse travelled 200 mm. The equation for computing UPV value is given below:

$$\text{UPV} = l/t \tag{1}$$

in which, the unit of UPV is in kilometres per second,

l denotes the length of the specimen

t is the time taken by the pulse to travel along the whole length of the specimen.

2.4.2. Mechanical properties

ASTM C348 (2002) based three-point loading system was adopted for the determination of the flexural strength. The size for the beam specimens was 160 × 40 × 40 mm. The formula used for the determination of flexural strength is given as follows:

$$S_f = 0.0028\ P$$

where S_f denotes the flexural strength in MPa and

P denotes the maximum load in N.

For the determination of the compressive strength, ASTM C109-based guidelines were taken into consideration. Three identical cylindrical specimens were used for each test.

2.4.3. Water absorption tests

For determining the porosity of the specimens, the water absorption tests were performed according to ASTM C642-13 (2013). The dimensions of the cylindrical specimens were 100 × 50 mm. Three identical cylindrical specimens were used for each test.

2.4.4. Microstructural characterisation and spectroscopy analysis

More advanced testing was conducted at 90 days to gain more in-depth understanding on their microstructure. The sample was kept inside an enclosed chamber for an electron beam to strike it. An electron microscope was used in this examination. A contrast detector was used for the backscattered electrons which provides a contrast between various chemical constituents and a clear SEM image is produced.

EDS analysis was also performed for wavelength differentiation. An energy dispersive detector was used for this purpose which analyses X-Ray radiations. Afterwards, XRD analysis was conducted which monitored the scattering angles and intensity of the X- Rays emitted by the sample (Kim et al., 2012). For this purpose, the sample was first bombarded with X- Rays. A curve was then plotted between the angle of scattering and the values of intensities obtained.

FTIR analysis was carried out according to ASTM E1252 (2013). The purpose of this test is to detect the organic compounds inside the mixture produced. In this analysis, compounds containing carbon and hydrogen can be distinguished. The specimen was powdered and kept in a cup inside a diffuse reflectance device. The output was obtained in the form of an infrared spectrum.

3. Results and discussions

3.1. Water absorption

The water absorption test was performed to evaluate the outcome of geopolymerization on the pore structure of fly ash and WMP-based geopolymer matrix. Accordingly, the effect of marble replacement on the water absorption of geopolymer mortar was also examined. The tests were carried out after a curing period of 7, 14 and 28 days, and the results are presented in **Fig. 3**. In general, the water absorption of all the mixes did not change significantly, varying within the range of 1.98% to 2.36% for all the investigated ages.

The least water absorption was observed by the control mix without marble powder inclusion (100F0M) for all ages. From the results, it was observed that the water absorption of WMP-

based geopolymer mortar for all curing ages only slightly increased as compared to the control mortar. Meanwhile, other mixes also showed a similar range with a bit higher value of the water absorption. The percentage of water absorption at 28 days of all the geopolymer mortar mixes ranged from 1.98% to 2.24%. Since the average particle size of WMP is smaller than FA, it creates a closed packing density by filling the micro-pores in the matrix. However, non-reacted particles of marble waste, which are presented later, did not participate in the polymerisation. Therefore, these remained non-reacted particles did not improve the denseness of the microstructure in the matrix.

When comparing the 7-day water absorption of mixes 95F05M, 90F10M, 85F015 and 80F020M with 100F0M, an increment of 3.33%, 6.66%, 8.57% and 12.38% respectively was noticed. This may be due to the immaturity of the specimen since waste marble creates a hindrance due to its non-reactive particles in the polymerisation process. This trend was similar for all the investigated curing periods. Meanwhile, the specimens cured at 28 days showed marginally lower water absorption percentages. This can be attributed to the additional polymerisation of fly ash with time and the development of geopolymer gel around unreacted waste marble powder particles. Despite all the facts, the water absorption percentage of mixes 95F05M, 90F10M and 85F15M was lower than 3% at all ages, and it justifies the presence of WMP in the geopolymer mortar did not considerably increase its water absorption.

In general, the addition of marble powder had two opposing effects in geopolymer formation. First it decreases available aluminosilicate precursor content, which decreases strength. Secondly, marble particles worked as extra fine un-reactive aggregates and provide a suitable nucleus for the formation of a network of interlinked polymer chains. Marble particles failed to form interfacial transition zone (ITZ) with GPM matrix, but due to WMP pore-filling effect, the GPM pore structure did not degrade considerably as evidenced by only a marginal increase in the water absorption.

Yamanel et al. (2019) revealed that inert marble dust as cement mass replacement (5, 10, 15 and 20%) did not contribute to hydration of mortar mixture. Furthermore, marble dust increased the porosity and hence the water absorption capacity from 6% in the reference mix to 8% in the mix with the highest marble content. Another study (Komnitsas et al. 2021) showed that the water absorption increased by 25.66% when 30% WMP was used as a binder substitute in metakaolin-based GPM. These results from the previous studies showed the similar influence of WMP on the water absorption.

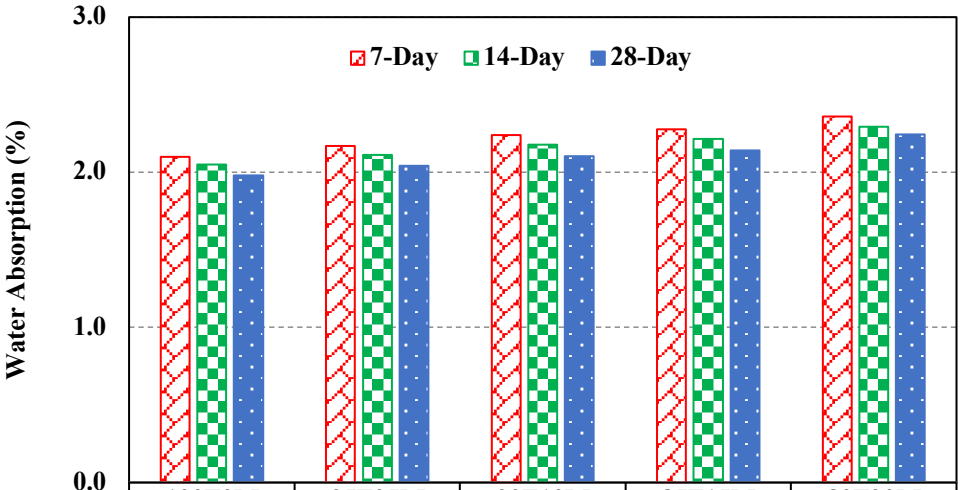

	100F0M	95F05M	90F10M	85F15M	80F20M
7-Day	2.10	2.17	2.24	2.28	2.36
14-Day	2.05	2.11	2.18	2.21	2.29
28-Day	1.98	2.04	2.11	2.14	2.24

Fig. 3. Percentage water absorption of geopolymer mortar mixes at various ages.

3.2.Ultrasonic pulse velocity test

The ultrasonic pulse velocity test (UPV) was performed to measure the stress wave velocity in the specimens and thus examine the internal structure of geopolymer matrix. Assessment of cracks and their bonding ability with WMP can be assessed by UPV. Mean UPV values for each GP mix at distinct ages are shown in **Fig. 4**. Evaluating the speed of ultrasonic pulses travelling through geopolymer matrix made with/without marble powder provides a good indication for denseness of the microstructure. It was observed that UPV of geopolymer mortar made up solely of fly ash as source material was higher than other mixes with WMP inclusion. Meanwhile, an increase in UPV values was observed in all the mixes with respect to curing ages, which ensures the progressive formation of internal structure with ages. At 7 days, the UPV of mixes 95F05M, 90F10M, 85F15M and 80F20M reduced by of 12%, 18.2%, 24.34% and 32.38% as compared to that of 100F0M, respectively. A similar trend was observed for 14-day cured specimens.

From the test results, it was observed that the 28-day UPV of mixes 100F0M, 95F05M and 90F10M was respectively 4.59, 4.24 and 4.10 km/s and these values are categorised as excellent according to BS 1881–203 (1986) guidelines (**Table 6)**. The 28-day UPV performance for mixes 85F15M and 80F20M was observed as medium quality. The UPV of mixes 95F05M and 90F10M reduced respectively by 7.4% and 10.6% as compared to that of mix 100F0M, but fall in excellent category. The relatively poor performance of mixes

85F015M and 80F20M may be due to cavities created around excess un-reactive marble particles. In addition, the decease of UPV can be attributed to the reduction of the compressive strength of the mixes with WMP replacement. Marble powder is a substitution to binder content and its replacement leads to a reduction in the compressive strength (f_c), which is proportion to the modulus of elasticity (E_c). As a result, a reduction of the compressive strength leads to decrease in the elastic modulus but with a slower rate. The UPV test measures the velocity of stress wave in concrete, which can be calculated as $V = \sqrt{\frac{E_c}{\rho}}$, where ρ is the density of concrete. When the density of concrete remains almost unchanged or is expected to have a minor change, the UPV is proportional to the elastic modulus. Therefore, a decrease in the compressive strength of mortar led to a decrease in its UPV.

Similar finding was also reported by Seghir et al. (2020) who attributed the decline in UPV (3.16% with 15% marble replacement) to the increased porosity and reduced hydrate products in cement-based mortar, when incorporating WMP as a binder substitute.

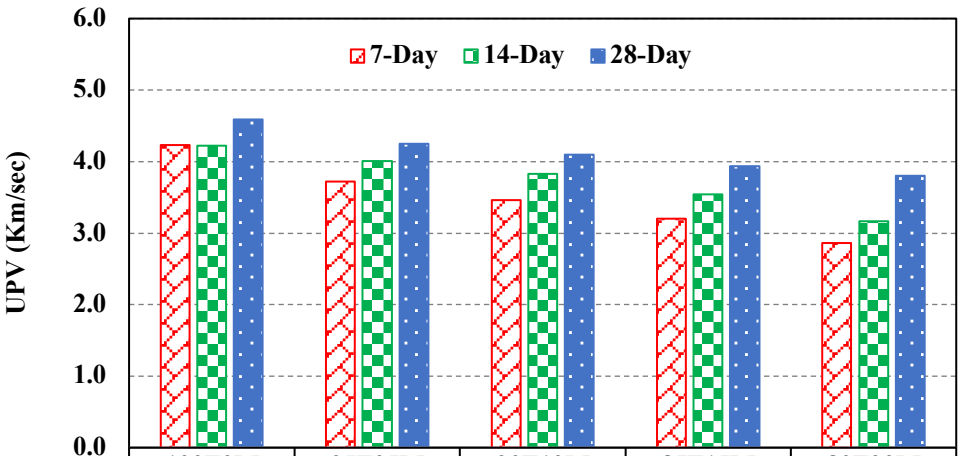

	100F0M	95F05M	90F10M	85F15M	80F20M
7-Day	4.23	3.72	3.46	3.20	2.86
14-Day	4.22	4.01	3.83	3.54	3.17
28-Day	4.59	4.25	4.10	3.94	3.80

Fig. 4. Ultrasonic pulse velocity of geopolymer mortar mixes at various ages.

Table 5. Quality Interpolation from UPV

Age	Average Ultrasonic Pulse Velocity (km/Sec)				
	100F0M	95F05M	90F10M	85F15M	80F20M
28-day	4.591	4.248	4.103	3.941	3.799
Quality	Excellent	Excellent	Excellent	Medium	Medium

3.3.Compressive strength

The compressive strength of all the mixes at 7, 14 and 28 days is presented in **Fig. 5**. Each result of the compressive strength is the average of three identical specimens tested at different ages. All the comparisons are made with reference to the control mix, 100F0M. Irrespective of age, the compressive strength of the reference mix, 100F0M, was greater than all the other mixes. The 7-day compressive strength of mixes 95F5M, 90F10M, 85F15M and 80F20M reduced by 3.68%, 6.90%, 10.86% and 18.97 % as compared to that of mix 100F0M, respectively. The corresponding compressive strengths at 14 and 28 days also revealed the same trend. Mixes 95F5M and 90F10M exhibited the 28 days compressive strength comparable to that of the control mix (24.95 MPa). Although mix 80F20M showed a remarkable decrease in the 28-day strength, by 4.24 MPa as compared to the control mix, but percentage wise the 28 days strength reduction (16.9%) is less than the results of 7 days testing (18.97%). This observation indicates that marble powder delayed strength development at early stages of geopolymer formation. The compressive strength reduced as the replacement level of marble powder increased suggested that marble particles served primarily as fillers and they did not effectively participate in geopolymer reaction, which is further confirmed by XRD and FTIR analyses. Furthermore, marble powder used as a replacement for fly ash (5-15%) resulted in about 4-17% decrease in the compressive strength at 28 days.

Temuujin et al. (2010) explained that the compressive strength of geopolymer mortar remains essentially same for varying sand aggregate content because the strength of mortar primarily depends on strength of hardened geopolymer gel. Therefore, a decrease in the compressive strength of GPM due to marble powder addition is a result of less geopolymer gel formation and poor interfacial bonding between inert marble particles and geopolymer gel. Also marble particles themself possess weaker mechanical properties than geopolymer gel and natural aggregates. The compressive strength of geopolymer mortar primarily depends on volume and strength of geopolymer gel and aggregates, and the bond between aggregates and geopolymer gel.

The fly ash content in geopolymer decreases with an increase in marble powder content which results in increased AAL to fly ash ratio and increases the probability of dissolution of fly ash for complete geopolymerisation. However, a previous study indicated that each fly ash patch has a different optimum Al/FA ratio to achieve complete activation depending on fly ash fineness and amorphous content (Hadi et al. 2018). Based on preliminary studies done in this

study the AAL content of 0.45 was sufficient for dissolution of fly ash and any further increase would not lead to the formation of additional geopolymeric gel and increase in GPM strength (Hardjito et al. 2004).

The compressive strength pattern obtained in this study is in agreement with an existing study by Komnitas et al. (2021) who used WMP as binder replacement in metakaolin-based geopolymer mortar. The decrease in the compressive strength of specimens with an increase in waste MP to metakaolin mass ratios of 0.3, 0.7 and 1.5 was found to be 20.41%, 36.1% and 60%, respectively; and was attributed to poor alkali activation potential of marble powder.

At 28 days, the compressive strength of mixes 95F05M, 90F10M, 85F15M and 80F20M reduced by 3.48%, 6.77%, 11.86% and 16.99% as compared to that of mix 100F0M, respectively. From these results, an empirical equation can be derived to estimate the compressive strength of the mix at 28 days as follows:

$$f_c = 25 - 16.98\ (\mathrm{WMP/FA}) \qquad R^2 = 0.977$$

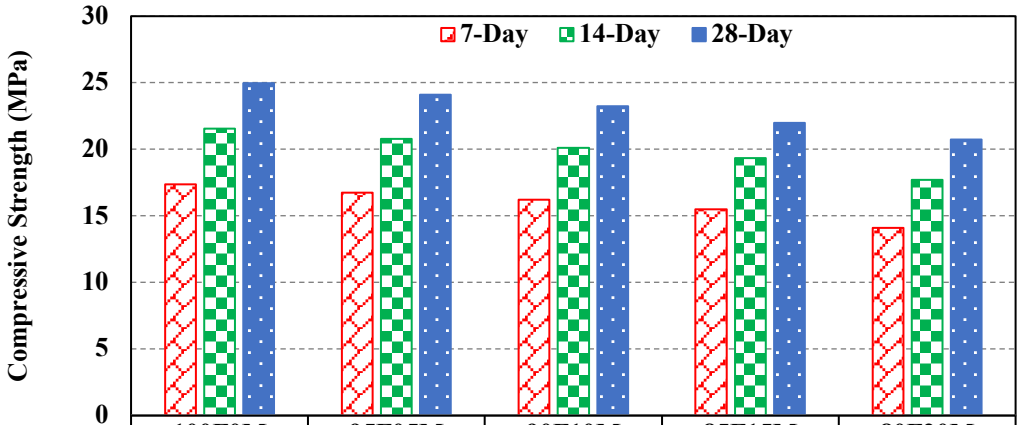

	100F0M	95F05M	90F10M	85F15M	80F20M
7-Day	17.39	16.75	16.19	15.50	14.09
14-Day	21.56	20.79	20.10	19.33	17.68
28-Day	24.95	24.08	23.26	21.99	20.71

Fig. 5. Compressive strength of geopolymer mortar mixes at various ages.

3.4.Flexural Strength

Fig. 6 depicts the flexural strength of the beam specimens for all the mixes at 7, 14 and 28 days. The results reveal that the flexural strength of mix 100F0M was also the highest among all the other mixes. Therefore, it could be inferred that fly ash plays a vital role in geopolymer

mortar while marble powder was not effective in gaining strength. Irrespective of the curing period, the flexural strength of mix 95F05M was found almost similar to the control mix. The minimum flexural strength was observed in mix 80F20M, e.g., its flexural strength at 7, 14 and 28 days was 1.92, 2.14 and 2.30 MPa, respectively. At 28 days, the flexural strength of mixes 95F05M, 90F10M, 85F15M and 80F20M decreased by 1.73%, 3.47%, 6.08% and 9.13% regarding mix 100F0M, respectively. This in the flexural strength may be due to the poor bonding of marble particles with GPM matrix. The reduction in flexural strength results was due to higher porosity of the interfacial transition zone (ITZ) with marble particles. Although, the flexural strength of a mortar is directly related to its performance under compressive load, strength reduction percentage in flexure was less as compared to its compressive strength.

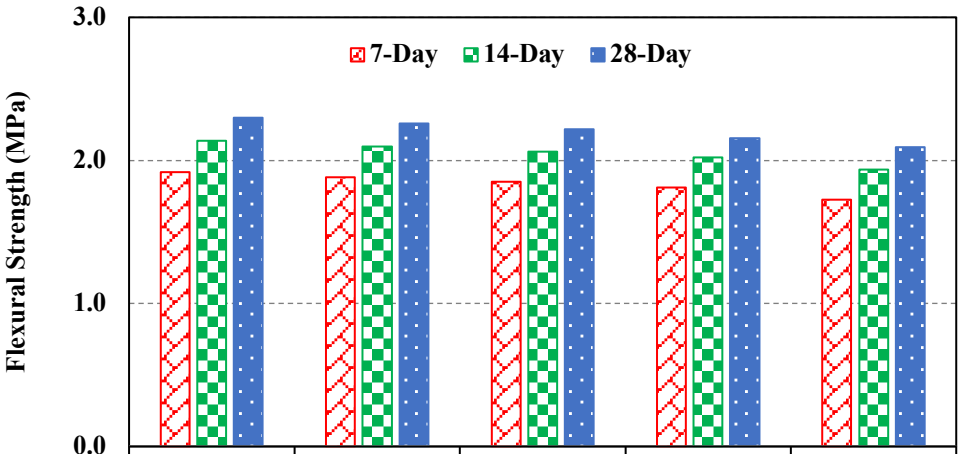

	100F0M	95F05M	90F10M	85F15M	80F20M
7-Day	1.92	1.88	1.85	1.81	1.73
14-Day	2.14	2.10	2.06	2.02	1.93
28-Day	2.30	2.26	2.22	2.16	2.09

Fig. 6. Flexural strength of geopolymer mortar mixes at various ages.

3.5.SEM and EDS analyses

Scanning electron microscopy (SEM) examination was conducted after 28 days and the resulting images are shown in **Fig. 7**. SEM images were used to investigate the GPM microstructure in detail and the bonding characteristics between geopolymer matrix and marble powder. At the microscopic level the matrix appears to be homogenous which suggests that unreactive micro-sized marble particles get evenly distributed in the GPM matrix. A close inspection of the interfacial region suggests negligible dissolution of the WMP particles which result in almost non-existent bond between marble particles and geopolymer binder. So, it can be concluded that the marble powder was mostly unreactive in geopolymer as no sufficient

bond was formed with the matrix. Due to weak adhesion with geopolymer gel, the marble particles act merely as void fillers but did not affect the mortar matrix homogeneity significantly. The SEM image of 100F0M shows that the control GPM mix, without marble powder, had more compact and homogenous structure when compared to the SEM image of the other mixes with marble powder replacement. The SEM images of mixes 95F05M, 90F10M, 85F15M and 80F20M show a higher degree of pores, unreacted particles and frequent micro cracks, which justifies their high water absorption and low strength performance. Fine marble particles which affect the geopolymer gel formation and the weaker inter-transition zone is found in SEM images of mixes 85F015M and 80F20M.

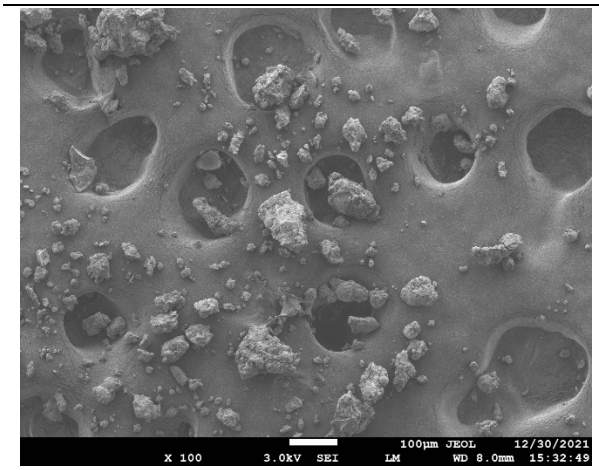

(a) Compact and homogenous microstructure of 100F0M

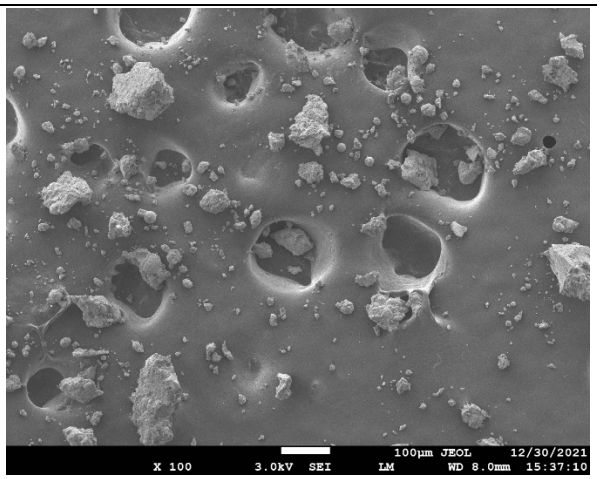

(b) Even distribution of marble particles in the 95F05M matrix

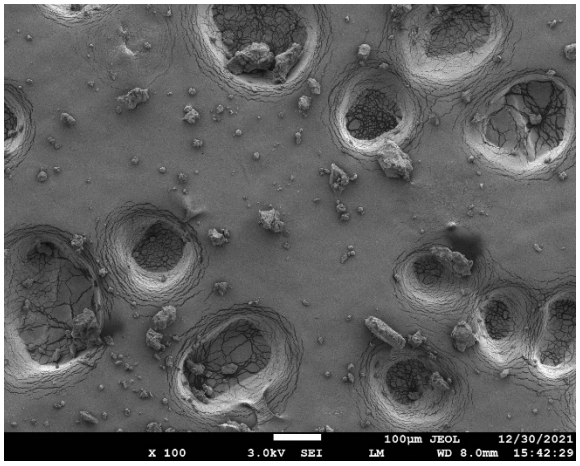

(c) Porous structure observed in 90F10M

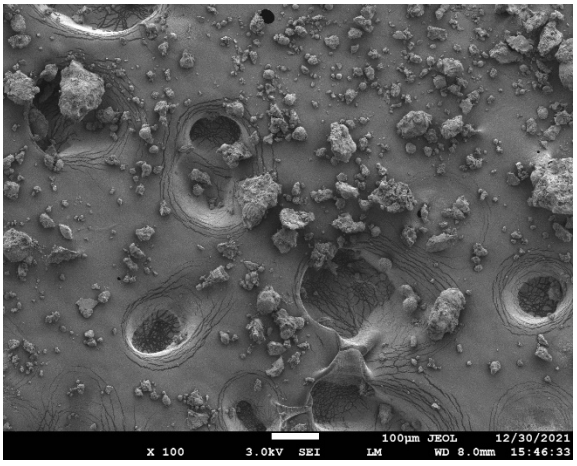

(d) Early signs of micro-cracking in 85F15M

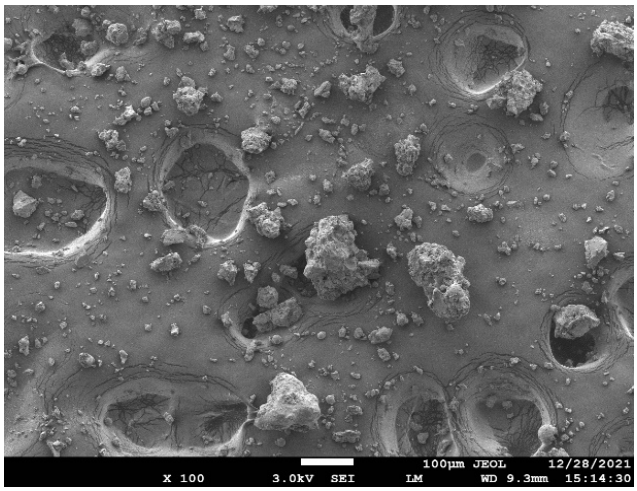

(e) Unreacted marble particles in 80F20M

Fig. 7. SEM images of all the mixes.

Fig. 8 present**s** the microstructural investigations using EDS tests, which show that Na, Al and Si make up the majority of the glassy matrix in all the GPM mixes and are the essential constituents of a geopolymer gel. According to the elemental atomic ratios of GPM calculated in **Table 8**, the geopolymeric matrix's Si/Al ratio slightly reduces with WMP replacement percentage, which has a detrimental effect on the development of geopolymer gel (Duxson et al. 2007; Wang et al. 2020). It is because when incorporating WMP, the fly ash content decreases and AAL/FA ratio increases, which leads to a decrease in dissolution of unreacted fly ash particles and release of less aluminosilicates in the geopolymer gel. The Ca/Si ratio shows a marginal decrease with the WMP content, which proves that the incorporated marble particles were almost unreactive in surrounding alkaline media and did not produce significant calcium ions in the geopolymer mix. Furthermore, the carbon compounds percentage increases from 8.91% to 16.07% (**Table 8**) due to carbonation of excessive alkaline solution, as AAL/FA ratio increases.

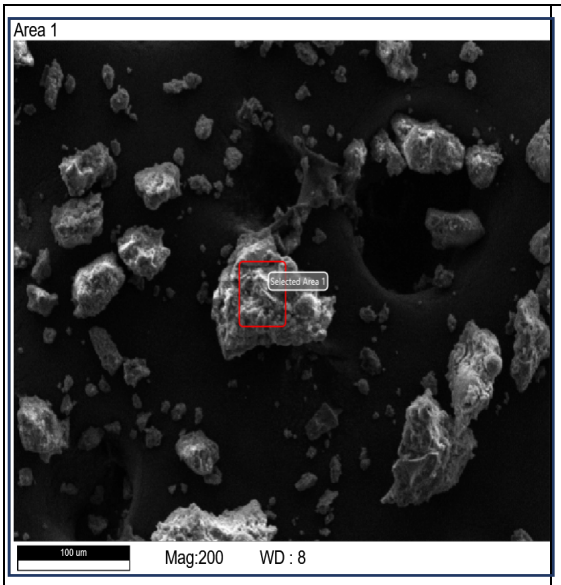

(a) 100F0M at 28 days

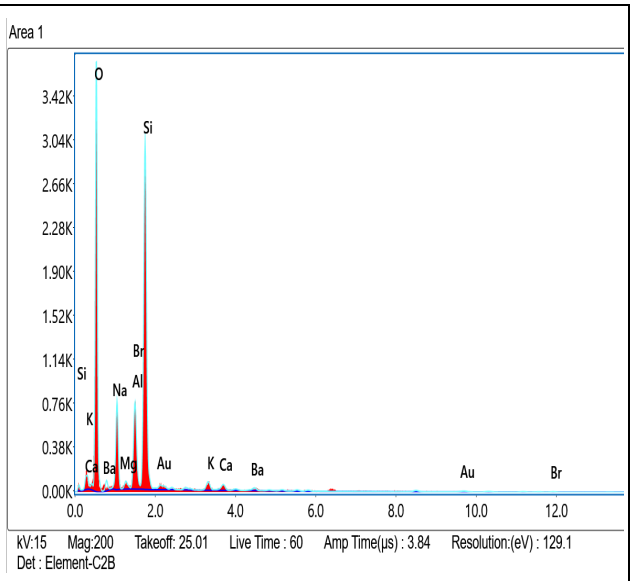

EDS analysis at 28 days (100F0M)

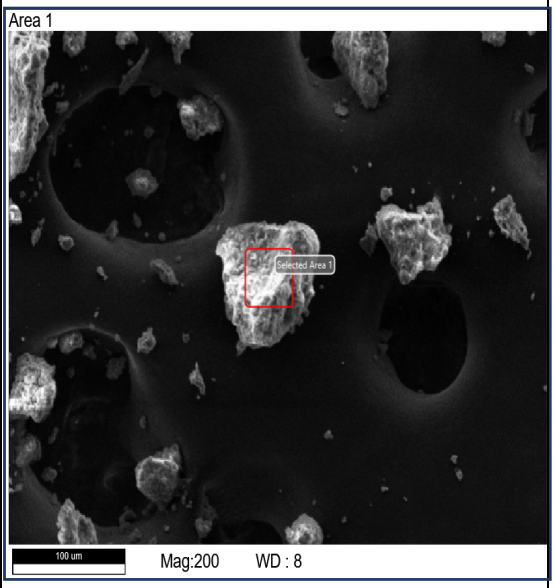

(b) 95F5M at 28 days

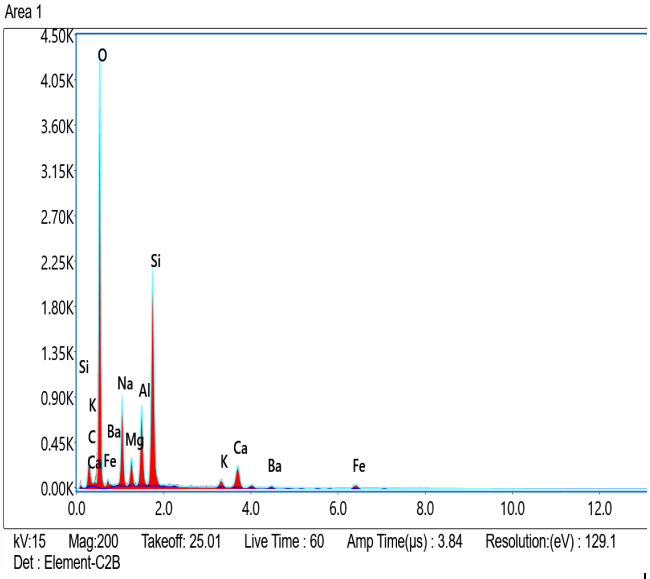

EDS analysis at 28 days (95F5M)

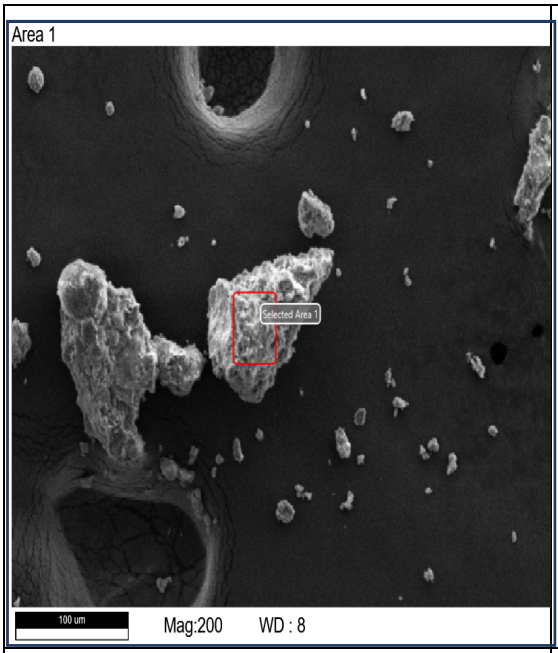

(c) 90F10M at 28 days

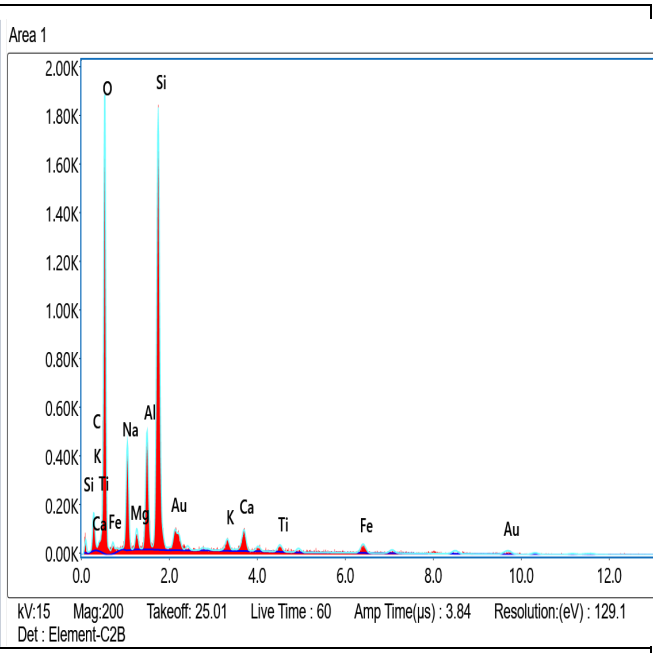

EDS analysis at 28 days (90F10M)

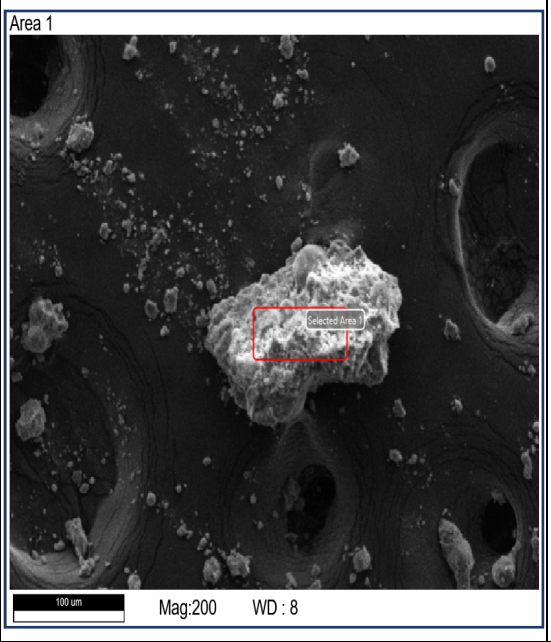

(d) 85F15M at 28 days

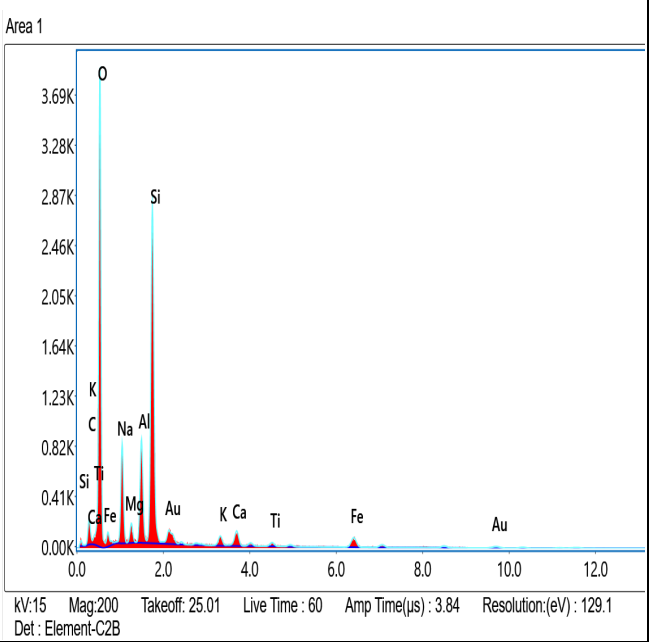

EDS analysis at 28 days (85F15M)

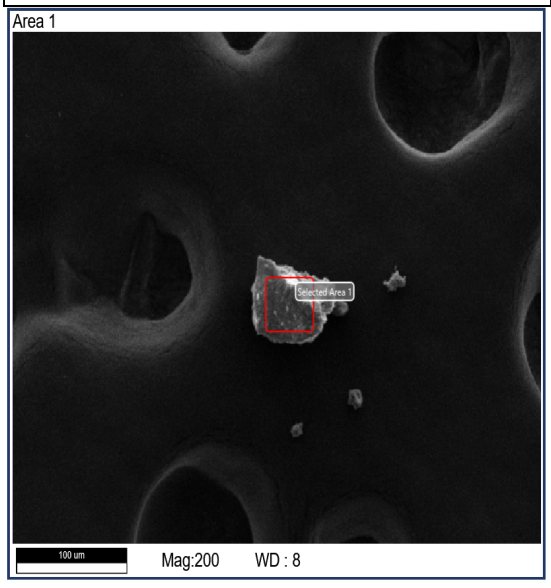

	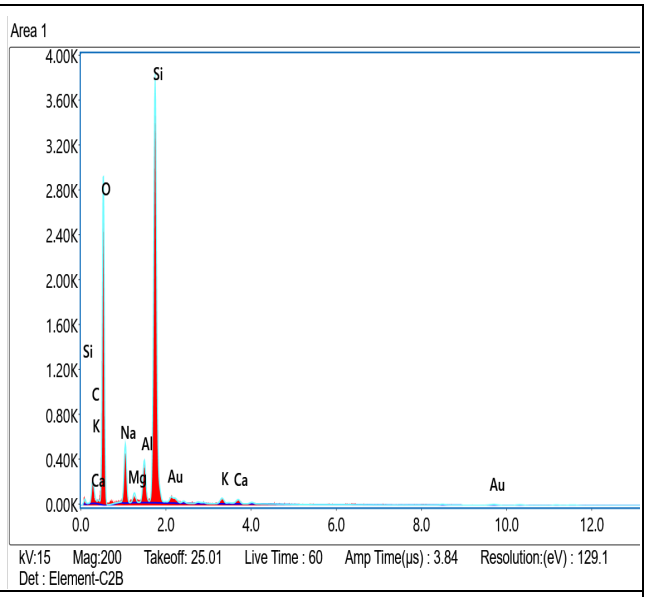
(e) 80F20M at 28 days	EDS analysis at 28 days (80F20M)

Fig. 8. EDS analysis results (Note: Needles at Ca and Si)

Table 6. Atomic ratios of elements.

	100F0M	95F05M	90F10M	85F15M	80F20M
Element	Atomic (%)	Atomic (%)	Atomic (%)	Atomic (%)	Atomic (%)
C K	8.91	10.21	12.98	14.53	16.07
O K	56.07	55.8	53.8	52.26	52.21
Na K	9.56	8.93	7.91	7.84	6.88
Mg K	1.51	1.94	1.34	1.18	0.83
Br L	1.69	0.77	1.15	0.29	0.78
Al K	4.23	4.32	4.39	4.68	4.81
Si K	12.45	12.42	12.43	13.01	13.36
Au M	0.1	0.1	0.37	0.57	0.14
K K	0.76	0.6	0.67	0.65	0.48
Ca K	3.59	3.52	3.39	3.21	3.14
Ba L	0.32	0.23	0.16	0.31	0.16
Ti K	0.42	0.37	0.52	0.63	0.43
Fe K	0.39	0.79	0.89	0.84	0.71
Ca/Si	0.288	0.283	0.273	0.247	0.235
Si/Al	2.943	2.875	2.831	2.780	2.778

3.6.X-Ray Diffraction (XRD)

The existence of distinct phases in GPM specimens after 28 days was determined by XRD analysis as shown in **Fig. 9**. The crystalline content of a sample produces sharp diffraction peaks when bombarded with X-rays. The control GPM mix shows the presence of crystalline

minerals which were intrinsic phases of the aluminosilicate raw material used, as crystalline components are incapable of dissolution in the polymerisation reaction. Crystalline phases such as mullite, nepheline and albite are common to both fly ash and its geopolymer mortar. These crystalline feldspar minerals are composed of aluminate compounds. The absence of mullite and quartz peak near 32° and 51°, respectively, in control GPM was due to higher dissolution of fly ash and consumption of amorphous silica in the alkaline media. From the XRD results, it is inferred that the presence of quartz was dominant in all the mixes. Quartz mineral peaks in the control GPM were due to the crystalline silica component of fly ash and natural fine aggregates. The dispersion peaks in the region of 22° to 36° are the characteristic amorphous substances in geopolymer. This broad hump in **Fig. 9** is noticeably displaced to the right in comparison to the XRD patterns of fly ash in **Fig. 1 (a)** (12° to 28°), indicating the production of new amorphous substances (Na-Al-Si-H) in the geopolymer reaction products.

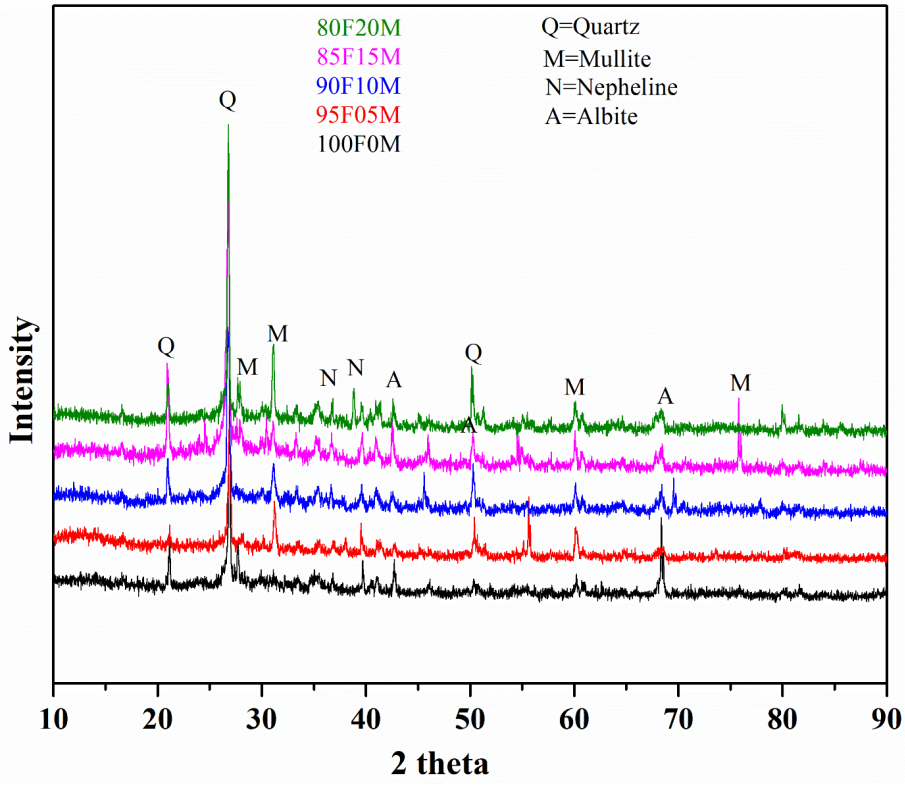

Fig. 9. XRD graphs of geopolymer mortar specimens

Furthermore, the position and size of dispersion peaks of reaction products of each mix were similar, implying that the degree of polymerisation and reaction products were relatively the same for WMP-based GPM. By comparing different phases present in XRD graphs of fly ash-based geopolymer control mix and its engineered mortar mixes, it is clear that there were no peaks and humps that indicate the presence of calcium-based compounds in GPM mortars. Thus, using marble powder as a partial substitute for fly ash did not alter the phase composition

qualitatively. However, marble powder did change the phase ratios. It is evident from the XRD results that marble powder primarily remains inert to the alkaline activator solution and lacks potential to take part in the geopolymerisation reaction. Komnistas et al. (2021) also reached to similar conclusion while inspecting the valorization potential of marble powder through alkali activation.

3.7. Fourier Transform Infrared Spectroscopy (FTIR)

FTIR analysis report can be seen in **Fig. 10**. During the geopolymerisation reaction of the control mix, 100F0M, the Si–O–Si/Si–O–Al bending band can be seen at 440 cm^{-1}, while the band at 542 cm^{-1} appears due to AlO^{4-} vibrations. The band at 1019 cm^{-1} is due to asymmetric stretching of Si–O and Al–O bonds resulting from dissolution of precursor fly ash. The relatively weak band at 1385 cm^{-1} represents stretching vibration of CO_3^{2-} ion. This peak becomes more noticeable when WMP is introduced in the GPM mix due to the presence of $CaCO_3$ in marble. This observation further establishes that the calcium content of marble remains bound, which renders it impotent to form new bonds with geopolymer gel. In all the geopolymeric mixes, bands in the regions of 1640 and 3440 cm^{-1} which were attributed to bending vibrations (H–O–H) and stretching vibration (–OH), respectively and represent the bound water present in the polymerisation products (Hou et al. 2009). Bound water molecules were largely adsorbed on the geopolymer gel surface and some were trapped in the GPM cavities.

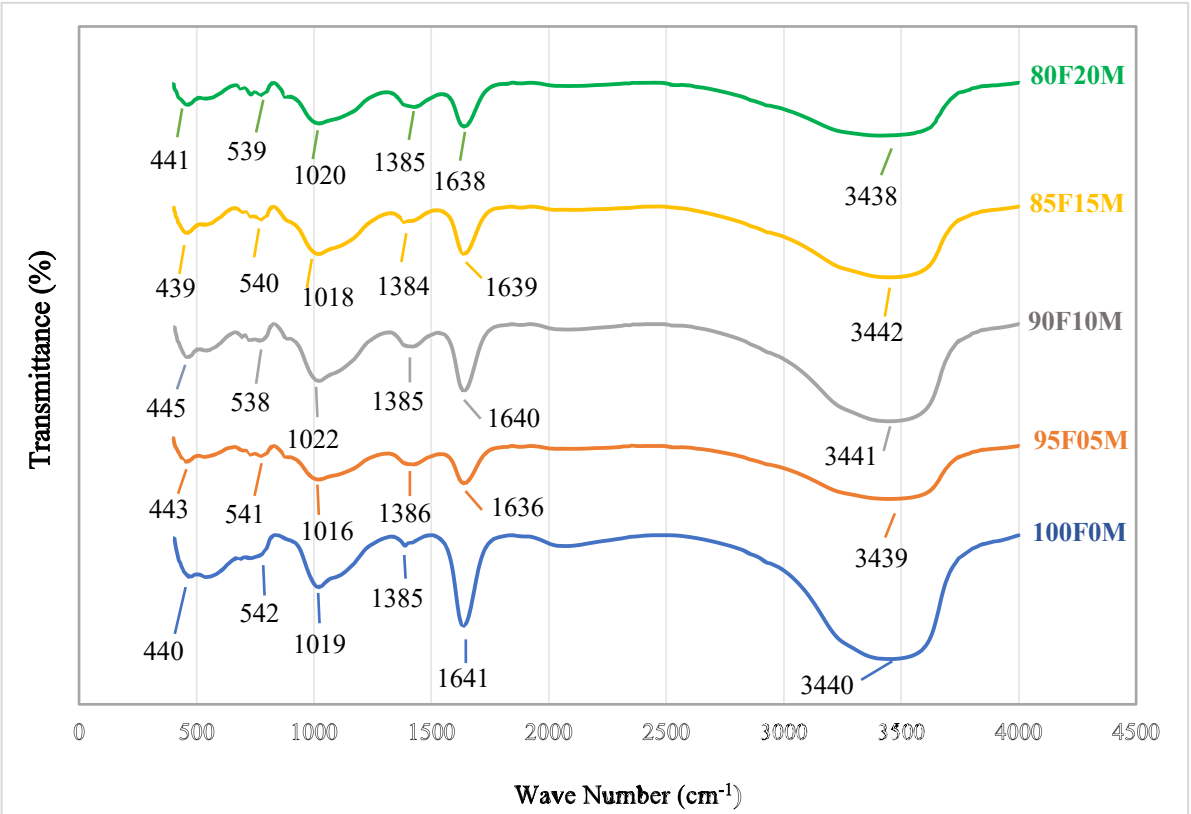

Fig. 10. FTIR spectra of each geopolymer mortar mix.

All the above bands are indicative of the formation of the aluminosilicate network in a geopolymer gel. It is quite complex to determine the extent of geopolymerization based on location and intensity of these bands, but their presence is solely due to the presence of amorphous phase of the alumino-silicate raw material.

It can be observed that GPM mixes with marble powder addition did not display new peaks, which indicates that marble powder has not formed additional chemical bonds with geopolymer matrix and acts as a completely inert ingredient.

4. Conclusions

This study examined the feasibility of WMP as binder supplement in fly ash-based GPM based on mechanical performance and microstructural investigations. Following main conclusions can be made:

1. With an increase in WMP replacement, the water absorption increased as high specific surface area of WMP and unreacted marble particles introduced additional void volume in the matrix. However, all mixes showed a satisfactory WA percentage of less than 3%.
2. The decrease in UPV values with WMP is attributed to reduction in geopolymer gel volume proportion that deteriorated the overall matrix denseness and strength. However, after 28 days all the specimens exhibited UPV values which were classified well above the medium quality mortar.
3. Replacement of FA with WMP consistently reduced the compressive and flexural strength of GPM, due to WMP inability to contribute to geopolymer gel formation.
4. Further, 28 days compressive strength of all the mortar mixes prepared in this study, was above 20 MPa which could be used to make masonry mortar bricks and non-traffic pavement blocks, as per strength requirements of IS 2250 (1981) and IS 15658 (2006).
5. SEM images show unreacted WMP particles occupying interstitial spaces. Further, EDS analysis shows a marginal decrease in Ca/Si ratio with increasing WMP content, which revealed that WMP remained unreactive in surrounding alkaline media and did not produce additional calcium compounds. The percentage of carbon compounds increased with WMP/FA ratio, which could be attributed to carbonation of unused alkaline solution.
6. FTIR and XRD examinations confirmed that WMP has no noticeable role in geopolymerisation process and acted as a mere filler material, since no new compounds and chemical bonds were revealed during these microstructural studies.

Based on mechanical test results and microstructural analyses conducted in this study, it is suggested that WMP integrated GPM at low content (<20%) can find sustainable applications in various construction activities without significant reduction in mechanical strength.

Compliance with Ethical Standards and Competing interests

☒ The authors declare that they have no known competing financial interests or personal relationships that could have appeared to influence the work reported in this paper.

REFERENCE

Alam, J., & Akhtar, M. N. (2014). Fly ash utilization in different sectors in Indian scenario. *International Journal of Emerging Trends in Engineering and Development*, *1*(August 2011).

Aliabdo, A. A., Abd Elmoaty, A. E. M., & Auda, E. M. (2014). Re-use of waste marble dust in the production of cement and concrete. *Construction and Building Materials*, *50*, 28–41. https://doi.org/10.1016/j.conbuildmat.2013.09.005

Anuradha, R., Sreevidya, V., Venkatasubramani, R., & Rangan, B. V. (2012). Modified guidelines for geopolymer concrete mix design using Indian standard. *Asian Journal of Civil Engineering*, *13*(3), 353–364.

Arel, H. S. (2016). Recyclability of waste marble in concrete production. *Journal of Cleaner Production*, *131*, 179–188. https://doi.org/10.1016/j.jclepro.2016.05.052

Ashish, D. K. (2018). Feasibility of waste marble powder in concrete as partial substitution of cement and sand amalgam for sustainable growth. *Journal of Building Engineering*, *15*(December 2017), 236–242. https://doi.org/10.1016/j.jobe.2017.11.024

Ashish, D. K. (2019). Concrete made with waste marble powder and supplementary cementitious material for sustainable development. *Journal of Cleaner Production*, *211*, 716–729. https://doi.org/10.1016/j.jclepro.2018.11.245

ASTM C348, A. (2002). Flexural strength of hydraulic-cement mortars. *American Society for Testing and Material*, *04*, 1–6.

ASTM C597. (2016). Standard Test Method for Pulse Velocity Through Concrete. *American Society for Testing and Materials, West Conshohocken, PA, USA.*, pp. 1–4. https://doi.org/10.1520/C0597-16

ASTM C618-12a. (2012). Standard Specification for Coal Fly Ash and Raw or Calcined Natural Pozzolan for Use in Concrete. *Annual Book of ASTM Standards*, 1–5. https://doi.org/10.1520/C0618

ASTM E1252. (2013). Standard Practice for General Techniques for Obtaining Infrared Spectra for Qualitative Analysis. *Annual Book of ASTM Standards*, *03*(Reapproved 2013), 1–13. https://doi.org/10.1520/E1252-98R13

ASTMC127. (2009). *Standard Test Method for Density , Relative Density (Specific Gravity*

), and Absorption of Coarse Aggregate. 1–7.

ASTMC29/C29M. (1997). *Standard Test Method for Bulk Density and Voids in Aggregate* (pp. 1–4). pp. 1–4.

ASTMC33-13. (2013). *Standard Specification for Concrete Aggregates*. 1–11. https://doi.org/10.1520/C0033

ASTMC535. (2009). *Standard Test Method for Resistance to Degradation of Large-Size Coarse Aggregate by Abrasion and Impact in the Los Angeles Machine*. *14*, 14–16.

ASTMC642-97. (1997). Standard Test Method for Density, Absorption, and Voids in Hardened Concrete. *ASTM International*, (March), 1–3.

BS1881-203. (1986). Part 203: Recommendations for measurement of velocity of ultrasonic pulses in concrete. *Journal (Royal Society of Health)*, *76*(8), 435–435. https://doi.org/10.1177/146642405607600807

BS812-110. (1990). Methods for determination of aggregate crushing value (ACV). *BRITISH STANDARD INSTITUTION*.

BS812-112. (2015). *Determination of Aggregate Impact Value*. (iv), 1–6.

Chatterjee, A. K. (2010). Indian fly ashes, their characteristics, and potential for mechano-chemical activation for enhanced usability. *2nd International Conference on Sustainable Construction Materials and Technologies*, 41–51.

Duxson, P., Fernández-Jiménez, A., Provis, J. L., Lukey, G. C., Palomo, A., & Van Deventer, J. S. J. (2007). Geopolymer technology: The current state of the art. *Journal of Materials Science*, *42*(9), 2917–2933. https://doi.org/10.1007/s10853-006-0637-z

Duxson, P., Mallicoat, S. W., Lukey, G. C., Kriven, W. M., & van Deventer, J. S. J. (2007). The effect of alkali and Si/Al ratio on the development of mechanical properties of metakaolin-based geopolymers. *Colloids and Surfaces A: Physicochemical and Engineering Aspects*, *292*(1), 8–20. https://doi.org/10.1016/j.colsurfa.2006.05.044

Dwivedi, A., & Jain, M. (2014). Fly ash – waste management and overview : A Review. *Recent Research in Science and Technology 2014*, *6(1)*(january), 30–35.

Ferdous, M. W., Kayali, O., & Khennane, A. (2013). A detailed procedure of mix design for fly ash based geopolymer concrete. *Proceedings of the 4th Asia-Pacific Conference on FRP in Structures, APFIS 2013*, (December), 11–13.

570 Ghani, A., Ali, Z., Khan, F. A., Shah, S. R., Khan, S. W., & Rashid, M. (2020). Experimental
571 study on the behavior of waste marble powder as partial replacement of sand in
572 concrete. *SN Applied Sciences*, *2*(9), 1–13. https://doi.org/10.1007/s42452-020-03349-y

573 Gill, P., Jangra, P., & Ashish, D. K. (2023). Non-destructive prediction of strength of
574 geopolymer concrete employing lightweight recycled aggregates and copper slag.
575 *Energy, Ecology and Environment*, 1–14.

576 Gill, P., Jangra, P., Roychand, R., Saberian, M., & Li, J. (2023). Effects of various additives
577 on the crumb rubber integrated geopolymer concrete. *Cleaner Materials*, *8*(December
578 2022), 100181. https://doi.org/10.1016/j.clema.2023.100181

579 Hadi, M. N. S., Al-azzawi, M., & Yu, T. (2018). Effects of fly ash characteristics and alkaline
580 activator components on compressive strength of fly ash-based geopolymer mortar.
581 *Construction and Building Materials*, *175*, 41–54.
582 https://doi.org/10.1016/j.conbuildmat.2018.04.092

583 Hardjito, D., Wallah, S. E., Sumajouw, D. M. J., & Rangan, B. V. (2004). Factors influencing
584 the compressive strength of fly ash-based geopolymer concrete. *Civil Engineering …*,
585 *6*(2), 88–93. Retrieved from http://www.freepatentsonline.com/article/Civil-
586 Engineering-Dimension/170455954.html

587 Hebhoub, H., Aoun, H., Belachia, M., Houari, H., & Ghorbel, E. (2011). Use of waste marble
588 aggregates in concrete. *Construction and Building Materials*, *25*(3).
589 https://doi.org/10.1016/j.conbuildmat.2010.09.037

590 Hou, Y., Wang, D., Zhou, W., Lu, H., & Wang, L. (2009). Effect of activator and curing
591 mode on fly ash-based geopolymers. *Journal Wuhan University of Technology,*
592 *Materials Science Edition*, *24*(5), 711–715. https://doi.org/10.1007/s11595-009-5711-3

593 Jindal, B. B., Parveen, Singhal, D., & Goyal, A. (2017). Predicting Relationship between
594 Mechanical Properties of Low Calcium Fly Ash-Based Geopolymer Concrete.
595 *Transactions of the Indian Ceramic Society*, *76*(4), 258–265.
596 https://doi.org/10.1080/0371750X.2017.1412837

597 Junaid, M. T., Kayali, O., Khennane, A., & Black, J. (2015). A mix design procedure for low
598 calcium alkali activated fly ash-based concretes. *Construction and Building Materials*,
599 *79*(January), 301–310. https://doi.org/10.1016/j.conbuildmat.2015.01.048

600 Kabeer, K. I. S., & Vyas, A. (2018). Evaluation of strength and durability of lean concrete

mixes containing marble waste as fine aggregate. *European Journal of Environmental and Civil Engineering*, *24*. https://doi.org/10.1080/19648189.2018.1471009

Kamseu, E., Akono, A. T., Rosa, R., Mariani, A., & Leonelli, C. (2022). Valorization of marble powder wastes using rice husk ash to yield enhanced-performance inorganic polymer cements: Phase evolution, microstructure, and micromechanics analyses. *Cleaner Engineering and Technology*, *8*(November 2021), 100461. https://doi.org/10.1016/j.clet.2022.100461

Kaya, M., Köksal, F., Bayram, M., Nodehi, M., Gencel, O., & Ozbakkaloglu, T. (2022). The effect of marble powder on physico-mechanical and microstructural properties of kaolin-based geopolymer pastes. *Structural Concrete*, (October), 1–20. https://doi.org/10.1002/suco.202201010

Khan, M. A., Khan, B., Shahzada, K., Khan, S. W., Wahab, N., & Ahmad, M. I. (2020). Conversion of waste marble powder into a binding material. *Civil Engineering Journal (Iran)*, *6*(3), 431–445. https://doi.org/10.28991/cej-2020-03091481

Kim, W., Suh, C. Y., Cho, S. W., Roh, K. M., Kwon, H., Song, K., & Shon, I. J. (2012). A new method for the identification and quantification of magnetite–maghemite mixture using conventional X-ray diffraction technique. *Talanta*, *94*, 348–352. https://doi.org/10.1016/J.TALANTA.2012.03.001

Komnitsas, K., Soultana, A., & Bartzas, G. (2021). Marble waste valorization through alkali activation. *Minerals*, *11*(1), 1–16. https://doi.org/10.3390/min11010046

Kumar, V., Singla, S., & Garg, R. (2020). Strength and microstructure correlation of binary cement blends in presence of waste marble powder. *Materials Today: Proceedings*, *43*(xxxx), 857–862. https://doi.org/10.1016/j.matpr.2020.07.073

Lee, W. H., Lin, K. L., Chang, T. H., Ding, Y. C., & Cheng, T. W. (2020). Sustainable development and performance evaluation of marble-waste-based geopolymer concrete. *Polymers*, *12*(9). https://doi.org/10.3390/POLYM12091924

Lezzerini, M., Luti, L., Aquino, A., & Gallello, G. (2022). Effect of Marble Waste Powder as a Binder Replacement on the Mechanical Resistance of Cement Mortars. *Applied Sciences (Switzerland)*, *12(9)*, 4481.

Lloyd, N. A., & Rangan, B. V. (2010). Geopolymer concrete with fly ash. *2nd International Conference on Sustainable Construction Materials and Technologies*, *7*, 1493–1504.

632 Mehta, A., & Siddique, R. (2017). Properties of low-calcium fly ash based geopolymer
633 concrete incorporating OPC as partial replacement of fly ash. *Construction and Building*
634 *Materials*, *150*, 792–807. https://doi.org/10.1016/j.conbuildmat.2017.06.067

635 Mehta, A., & Siddique, R. (2018). Sustainable geopolymer concrete using ground granulated
636 blast furnace slag and rice husk ash: Strength and permeability properties. *Journal of*
637 *Cleaner Production*, *205*, 49–57. https://doi.org/10.1016/j.jclepro.2018.08.313

638 Nath, P., & Sarker, P. K. (2015). Use of OPC to improve setting and early strength properties
639 of low calcium fly ash geopolymer concrete cured at room temperature. *Cement and*
640 *Concrete Composites*, *55*, 205–214. https://doi.org/10.1016/j.cemconcomp.2014.08.008

641 Nath, P., Sarker, P. K., & Rangan, V. B. (2015). Early age properties of low-calcium fly ash
642 geopolymer concrete suitable for ambient curing. *Procedia Engineering*, *125*, 601–607.
643 https://doi.org/10.1016/j.proeng.2015.11.077

644 Nikvar-Hassani, A., Manjarrez, L., & Zhang, L. (2022). Rheology, Setting Time, and
645 Compressive Strength of Class F Fly Ash–Based Geopolymer Binder Containing
646 Ordinary Portland Cement. *Journal of Materials in Civil Engineering*, *34*(1), 4021375.

647 Palomo, A., Grutzeck, M. W., & Blanco, M. T. (1999). Alkali-activated fly ashes: A cement
648 for the future. *Cement and Concrete Research*, *29*(8), 1323–1329.
649 https://doi.org/10.1016/S0008-8846(98)00243-9

650 Pappu, A., Thakur, V. K., Patidar, R., Asolekar, S. R., & Saxena, M. (2019). Recycling
651 marble wastes and Jarosite wastes into sustainable hybrid composite materials and
652 validation through Response Surface Methodology. *Journal of Cleaner Production*, *240*,
653 118249. https://doi.org/https://doi.org/10.1016/j.jclepro.2019.118249

654 Rangan, B. (2014). Fly Ash-Based Geopolymer Concrete Fly Ash-Based Geopolymer
655 Concrete. *Geopolymer Cement and Concrete*, *7982*(May), 68–106. Retrieved from
656 https://www.researchgate.net/publication/230717147

657 Saloma, Saggaff, A., Hanafiah, & Mawarni, A. (2016). Geopolymer Mortar with Fly Ash.
658 *MATEC Web of Conferences*, *78*, 1–6. https://doi.org/10.1051/matecconf/20167801026

659 Saloni, Parveen, Lim, Y. Y., Pham, T. M., Jatin, & Kumar, J. (2021a). Sustainable alkali
660 activated concrete with fly ash and waste marble aggregates: Strength and Durability
661 studies. *Construction and Building Materials*, *283*, 122795.
662 https://doi.org/10.1016/j.conbuildmat.2021.122795

663 Saloni, Parveen, Lim, Y. Y., Pham, T. M., Jatin, & Kumar, J. (2021b). Sustainable alkali
664 activated concrete with fly ash and waste marble aggregates: Strength and Durability
665 studies. *Construction and Building Materials*, *283*, 122795.
666 https://doi.org/10.1016/j.conbuildmat.2021.122795

667 Seghir, N. T., Benaimeche, O., Krzywínski, K., & Sadowski, L. (2020). Ultrasonic evaluation
668 of cement-based building materials modified using marble powder sourced from
669 industrial wastes. *Buildings*, *10*(3). https://doi.org/10.3390/buildings10030038

670 Singh, M., Choudhary, K., Srivastava, A., Singh Sangwan, K., & Bhunia, D. (2017,
671 September 1). A study on environmental and economic impacts of using waste marble
672 powder in concrete. *Journal of Building Engineering*, Vol. 13, pp. 87–95.
673 https://doi.org/10.1016/j.jobe.2017.07.009

674 Sinsiri, T., Chindaprasirt, P., & Jaturapitakkul, C. (2010). Influence of fly ash fineness and
675 shape on the porosity and permeability of blended cement pastes. *International Journal*
676 *of Minerals, Metallurgy, and Materials 2010 17:6*, *17*(6), 683–690.
677 https://doi.org/10.1007/S12613-010-0374-9

678 Surabhi. (2017). Fly ash in India : Generation vis-à-vis Utilization and Global perspective.
679 *International Journal of Applied Chemistry*, *13*(1), 29–52.

680 Temuujin, J., Riessen, A. Van, & Mackenzie, K. J. D. (2010). Preparation and
681 characterisation of fly ash based geopolymer mortars. *Construction and Building*
682 *Materials*, *24*(10), 1906–1910. https://doi.org/10.1016/j.conbuildmat.2010.04.012

683 Ushaa, T. G., Anuradha, R., & Venkatasubramani, G. S. (2015). Performance of self-
684 compacting geopolymer concrete containing different mineral admixtures. In *Indian*
685 *Journal of Engineering & Materials Sciences* (Vol. 22).

686 Vardhan, K., Goyal, S., Siddique, R., & Singh, M. (2015). Mechanical properties and
687 microstructural analysis of cement mortar incorporating marble powder as partial
688 replacement of cement. *Construction and Building Materials*, *96*, 615–621.
689 https://doi.org/10.1016/j.conbuildmat.2015.08.071

690 Vardhan, K., Siddique, R., & Goyal, S. (2019). Influence of marble waste as partial
691 replacement of fine aggregates on strength and drying shrinkage of concrete.
692 *Construction and Building Materials*, *228*, 116730.
693 https://doi.org/10.1016/j.conbuildmat.2019.116730

694 Wang, J., Ma, B., Tan, H., Du, C., Chu, Z., Luo, Z., & Wang, P. (2021). Hydration and
695 mechanical properties of cement-marble powder system incorporating
696 triisopropanolamine. *Construction and Building Materials*, *266*, 121068.
697 https://doi.org/10.1016/j.conbuildmat.2020.121068

698 Wang, Q., Ding, Z. Y., Da, J., Ran, K., & Sui, Z. T. (2011). Factors Influencing Bonding
699 Strength of Geopolymer-Aggregate Interfacial Transition Zone. *Advanced Materials*
700 *Research*, *224*, 1–7. https://doi.org/10.4028/www.scientific.net/AMR.224.1

701 Wang, Y., Liu, X., Zhang, W., Li, Z., Zhang, Y., Li, Y., & Ren, Y. (2020). Effects of Si/Al
702 ratio on the efflorescence and properties of fly ash based geopolymer. *Journal of*
703 *Cleaner Production*, *244*. https://doi.org/10.1016/j.jclepro.2019.118852

704 Yamanel, K., Durak, U., Ilkentapar, S., Atabey, I. I., Karahan, O., & Atiş, C. D. (2019).
705 Influence of waste marble powder as a replacement of cement on the properties of
706 mortar. *Revista de La Construccion*, *18*(2), 290–300.
707 https://doi.org/10.7764/RDLC.18.2.290

708 Yousuf, A., Manzoor, S. O., & Youssouf, M. (2020). Fly Ash : Production and Utilization in
709 India - An Overview. *Journal of Materials and Environmental Science*, *11*(6), 911–921.

710 Zhang, H. Y., Kodur, V., Wu, B., Cao, L., & Wang, F. (2016). Thermal behavior and
711 mechanical properties of geopolymer mortar after exposure to elevated temperatures.
712 *Construction and Building Materials*, *109*, 17–24.
713 https://doi.org/https://doi.org/10.1016/j.conbuildmat.2016.01.043

714 Zhao, J., Tong, L., Li, B., Chen, T., Wang, C., Yang, G., & Zheng, Y. (2021). Eco-friendly
715 geopolymer materials: A review of performance improvement, potential application and
716 sustainability assessment. *Journal of Cleaner Production*, *307*, 127085.
717 https://doi.org/https://doi.org/10.1016/j.jclepro.2021.127085

718